The International Journal of Advanced Manufacturing Technology (2021) 112:203–220
https://doi.org/10.1007/s00170-020-06359-7

ORIGINAL ARTICLE

Early prediction method for assembly precision of mechanical system and assessment of precision reliability

Xin Yang[1] · Yan Ran[2] · Zhichao Wang[1] · Zongyi Mu[1] · Genbao Zhang[2]

Received: 9 July 2020 / Accepted: 4 November 2020 / Published online: 18 November 2020

Abstract
Assembly precision is an important index, because it can ensure the quality of mechanical products and the final basis, and determine the overall performance of the products. In the early design stage, the prediction of assembly precision of schemes is significant. Therefore, considering part processing error, we proposed a prediction method for assembly precision of mechanical transmission system. Based on meta-action theory and small displacement torsor (SDT) model, common geometric elements were analyzed under multi-tolerance coupling and the error transfer of joint-surface for meta-action unit. Thus, we established the error model of joint-surface and qualitatively determined the potential error's accumulative transmission paths of transmission system. We also quantitatively built the assembly precision prediction model of transmission system combining with the Jacobian-Torsor method, and calculated the precision reliability value. Finally, the effectiveness was verified by an example of NC machine tool's transmission system. The method provides a way of thinking about solving the precision prediction and reliability evaluation of mechanical transmission systems in the early design stage and a basis for the final assembly precision prediction, simulation and testing of mechanical products.

Keywords Assembly precision · Error analysis · Prediction method · Precision reliability

1 Introduction

Assembly errors are formed by the cumulative transfer of multiple local error sources based on the topological structure of mechanical products [1–3]. However, the structure of mechanical products is often complex and changeable. Complex mechanical products often contain thousands of parts. The geometric elements and matching forms among parts are also various [4, 5]. Therefore, setting up a general assembly error analysis model has become an urgent problem to be resolved in the manufacturing industry. In this paper, the tolerance modeling is carried out for the machining errors of transmission system's parts firstly. Accurately describing the geometric elements is the key of tolerance modeling according to the tolerance value [6, 7]. Whitney [8] established the assembly error transfer model, who applied the homogeneous transformation matrix used for posture operation in robotics for assembly tolerance analysis. Zhou et al. [9, 10] set up the error transfer model and quality evaluation method based on the assembly sequence, solved the accumulated errors of assembly according to the error transfer paths. It realized the assembly precision calculation. Zhang [11] proposed a representation model of geometric errors based on Non-Uniform Rational BSplines (NURBS) surface. It can consider forming errors and characterize the altitude distribution of geometric errors on the machined surface. All these error modeling methods are based on the traditional component structure decomposition. It often used in whole electromechanical products, its practicability is limited. Therefore, it is necessary to propose an assembly error modeling method specific to mechanical transmission parts with more general and convenient calculation.

Second, the state space model of the assembly process is established to predict assembly precision, using differential motion vectors to describe the error state of the assembly process [12]. Wong et al. [13] proposed a precision prediction method based on gap connector and multidimensional vector ring. It analyzed the assembly errors caused by connection

✉ Yan Ran
20160702061t@cqu.edu.cn

[1] College of Mechanical Engineering, Chongqing University, Chongqing 400044, China

[2] State Key Laboratory of Mechanical Transmissions, Chongqing University, Chongqing 400044, China

gap, position deviation, geometric shape deviation and assembly position deviation, established multidimensional vector ring and vector equation of assembly, and realized the assembly precision prediction. Zhang et al. [14–16] proposed an assembly error prediction method for caused by parts' deformation. It comprehensively considered the errors caused by parts' machining errors and parts' deformation, and realized calculating assembly errors considering part deformation. However, the model has certain limitations. Due to these research methods do not clearly express the influence between the variance of each error component and the variance of assembly precision index.

As an important premise of assembly precision control technology, assembly precision prediction has important practical significance for product error compensation and tolerance optimization [17, 18]. Therefore, an assembly error modeling method for the meta-action unit of complex mechanical products has been presented. FMA is a new decomposition method which establishes a design model (FMA-DM) based on the mapping relationship of "function-motion-action" [19–21] initially in the assembly stage. It can better consider the dynamic performance of electromechanical products in the work state and enhance the design quality at the beginning of early design stage. Based on this theory, we analyzed the transmission, accumulation rules of errors in the assembly process, found out the error transfer paths and assembled precision model. Eventually, the precision prediction of meta-action unit has been realized. Section 1 proposes the SDT error modeling method of geometric elements. The research on error transfer property and the error accumulation paths among the parts in the meta-action unit is described in Section 2 and Section 3. In Section 4, the assembly precision prediction method of meta-action unit based on the Jacobian-Torsor method is then discussed in detail. In Section 5, an analysis of the gear meta-action unit from the transmission system is used to expound the process and the idea of the meta-action assembly precision prediction method based on the geometric error modeling of parts. The feasibility of the method was demonstrated. Section 6 concludes this paper.

2 Basic theory

2.1 Geometric element error modeling and variation interval solution of error component

In the SDT tolerance model, a rigid slight change expresses the geometric errors of the parts through the nominal surface. The ideal geometric elements are used to replace the actual geometric elements of the parts [22, 23]. Within the scope of this research, the variations of SDT describe the geometric elements' errors of parts.

In SDT model, constrained inequalities restrict the error components' movement of geometric elements in the variable interval and are determined by variable inequalities. In the actual machine process, the error components present a certain distribution law, because of various factors such as human, machine, material, method and ring [24, 25]. We mainly studied the actual distribution law under each error component obeys normal distribution and is independent of each other. According to the unqualified rate P of the constraint equation and the random characteristics of manufacturing error and corresponding component values, the actual distribution law of geometric elements' each error component parameter is deduced under the constraint inequality restriction to obtain the actual error variation interval of each component. The constraint function consists of linear components, because the error components of the geometric elements are independent with each other. The constraint function f also obeys normal distribution, such as

$$\begin{aligned} &f(\alpha,\beta,\gamma,u,v,w)\sim N\left(0,\sigma^2\right)\\ &\sigma^2=g\left(\sigma_\alpha^2,\sigma_\beta^2,\sigma_\gamma^2,\sigma_u^2,\sigma_v^2,\sigma_w^2\right) \end{aligned} \tag{1}$$

When the value of the constraint function f has a failure rate of p in the range of $[\boldsymbol{T}_{\min}, \boldsymbol{T}_{\max}]$, as shown below:

$$\boldsymbol{\sigma}=\frac{\boldsymbol{T}_{S\max}-\boldsymbol{T}_{S\min}}{2\boldsymbol{X}} \tag{2}$$

Where, $\boldsymbol{X}=\boldsymbol{\Phi}^{-1}\left(\mathbf{1}-\frac{\boldsymbol{p}}{\mathbf{2}}\right)$. Depending on the Eqs. (1) ~ (3), the distribution parameters of each error component under the constraint relationship can be obtained.

2.2 The Jacobian-Torsor variance model

The unified Jacobian-Torsor variance model is a three-dimensional tolerance model combining Jacobian matrix and the torsor variance model. It has drawn the attentions of many researchers. The Jacobian matrix is a linear arithmetic formulation, which derived from the description of kinematic chains in robotics. Displacements of FE pairs are very small in tolerance zones. So, they can also be transferred to the FR through Jacobian matrixes in assemblies, and it can express complex assembly relations. The Jacobian-Torsor variance model can be presented as

$$[FR]_{6\times1}=\sum_{i=1}^{n}[J_{FEi}]_{6\times6}^{2}[FE_i]_{6\times1} \tag{3}$$

Where, n is the number of features affect $[FR]$. $[FE]$ represents the influence degree of the variance of error component for each characteristic on the variance of error component for function requirement. In this paper, feature refers to the joint-surface.

Assuming that the error components are independent of each other, so the variance of the displacement error component and rotational error component are respectively:

$$\begin{bmatrix} \sigma^2_{\Delta x} \\ \sigma^2_{\Delta y} \\ \sigma^2_{\Delta z} \end{bmatrix} = \left(w_i^n\right)^2 \begin{bmatrix} \sigma^2_{\alpha} \\ \sigma^2_{\beta} \\ \sigma^2_{\gamma} \end{bmatrix} + \begin{bmatrix} \sigma^2_{u} \\ \sigma^2_{v} \\ \sigma^2_{w} \end{bmatrix} \tag{4}$$

$$\begin{bmatrix} \sigma^2_{\Delta\alpha} \\ \sigma^2_{\Delta\beta} \\ \sigma^2_{\Delta\gamma} \end{bmatrix} = \begin{bmatrix} \sigma^2_{\alpha} \\ \sigma^2_{\beta} \\ \sigma^2_{\gamma} \end{bmatrix} \tag{5}$$

Desrochers et al. [26] proposed matric model, the changes in the characteristics in the tolerance was described by homogeneous transformation matrix. The model contains a rotating matric and a moving matrix model. It has the perfect tolerance constraint characteristics and mathematical expression based with the theory about technologically and topo logically related surfaces technology and the topological related identities. Therefore, we can get the formula (6) to express the effect of variance of error component of feature i on assembly function requirement $\boldsymbol{FR}$. Due to it is an existing research results do not need to introduce further at this point. More detailed information about these matrixes can be found in [27–29].

$$[FR] = \begin{bmatrix} R_0^i & w_i^n R_0^i \\ 0 & R_0^i \end{bmatrix}^{\bullet 2} \begin{bmatrix} \sigma^2_{u} \\ \sigma^2_{v} \\ \sigma^2_{w} \\ \sigma^2_{\alpha} \\ \sigma^2_{\beta} \\ \sigma^2_{\gamma} \end{bmatrix} = [J_{FEi}]^{\bullet 2}[FE_i] \tag{6}$$

Where $[FR]$ is the variance of error component for function requirements. $[FE_i]$ is the variance of error component for characteristic i. As the Jacobian matrix is $[J_{FEi}]$, $[J_{FEi}]^2$ is now defined as the Jacobian variance matrix, and it is used to express the influence relationship degree of variance of error components of characteristic i.

3 Error transfer of the joint-surface of parts in meta-action unit

In engineering, multidisciplinary design optimization (MDO) has been widely applied to improve the performance of mechanical systems, which are often high-dimensional problems [30]. Therefore, reducing the dimensionality of the problem is a natural strategy to tackle this challenge. One of the strategies is to decompose the complex system into several subsystems of lower dimension [16], so the meta-action theory was proposed. It is an innovative and dynamic method to decompose electromechanical products by taking the meta-action unit as the minimum granularity, as shown in Figs. 1 and 2.

$$P = \langle F, M, A \rangle \tag{7}$$

Where P describes the function realization process, including function layer F, motion layer M, and meta-action layer A.

3.1 Error transfer properties of joint-surface of parts in meta-action unit

In the process of assembly, the positioning of parts is the constraint imposed on adjacent parts by joint surface. Meanwhile, the variation of error affects the positioning state of the adjacent parts, so the error is transmitted. The error transfer property of the joint-surface refers to that the joint-surface selectively transfers the error component of two geometric elements based on the matching characteristics among parts. It is closely related to the geometry of the joint-surface. Planar and cylinders are two common types of joint-surfaces [31], and their error transfer properties are given in Table 1.

Through multiple joint-surfaces, both composite and parallel joint-surfaces are controlled the error variation. The difference between them are the size of the positioned geometric elements relative to the parts. When each positioned geometric element of the part is relatively small, it belongs to the composite joint-surface. Otherwise, it belongs to parallel joint-surfaces. The common forms of joint-surface are also plane joint-surface and cylinder joint-surface in meta-action unit.

3.2 Error transfer mechanisms of parallel properties joint-surface in meta-action unit

There are several joint-surfaces in the meta-action unit. Through corresponding parts, they are correlated and interacted with each other, so as to form the error transfer system. According to the different relations in the transfer direction of adjacent joint-surfaces, the joint-surfaces can be divided into series joint-surfaces and parallel joint-surfaces, as shown in Fig. 3. The parallel joint-surfaces selectively transfer the error component of multiple geometric elements based on the matching characteristics among parts.

In Fig. 3, $P_1 - P_3$ are parts, F_1 and $F_2$are joint-surfaces, and arrows indicate the direction of the error transfer. The parts transmit errors through the joint-surface. The series joint-surfaces are the adjacent joint-surfaces that are single-channel serial at the error transfer direction, as shown in Fig. 3a. Similarly, the parallel joint-surfaces are the adjacent joint-surface of multi-channel parallel, as shown in Fig. 3b. According to the strength of the binding effect, the plane joint-surface can be divided into close fit and non-close fit, and the cylindrical joint-surface can be divided into interference fit and gap fit. When the plane joint-surface is a close fit or the cylindrical joint-surface is an interference fit, the direction of error transfer property is strongly constrained and the other direction is unconstrained. When plane joint-surface is

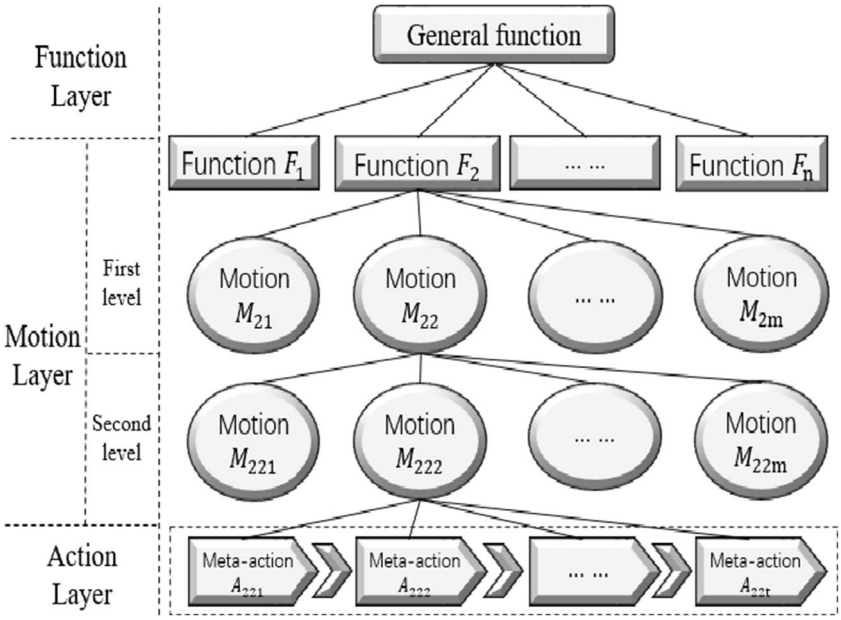

Fig. 1 FMA structured decomposition

non-close fit or the cylinder joint-surface is gap fit, the direction of error transfer property is weak constraint, and the others are unconstrained.

Assuming that the parallel joint-surface is composed of joint-surface 1 and 2, then we can define the strong constraint sets of parallel joint-surfaces, joint-surface 1 and joint-surface 2 are A_S, A_{1S}, and A_{2S}. The weak constraint sets of parallel joint-surfaces, joint-surface 1 and joint-surface 2 are A_W, A_{1W}, and A_{2W}. If there is no intersection among the constraint directions of the two joint-surfaces that make up the parallel joint-surfaces, the corresponding joint-surface transmits the error of the parallel joint-surfaces. Otherwise, the analysis of the actual error transfer properties of the parallel joint-surfaces can be divided into the following three situations:

(1) The parallel joint-surfaces are composed of two strong constraints. The two joint-surfaces have strong constraints in the same direction, which could cause entity interference and lead to assembly failure. Constraint strength of related binding surfaces should be adjusted.

(2) The parallel joint-surfaces are composed of strong constraint joint-surface and weak parallel joint-surfaces. The intersection of the two joint-surfaces with strong constraint and weak constraint is not empty. Assuming that joint-surface 1 is the strong constraint coordination, and 2 for the weak constraint coordination. Then, there is $A_{1S} \cap A_{2W} \neq \varnothing$. At this time, by adjusting the position of weak constraint direction, we can eliminate the entity interference. Then we can judge whether the entity interference can be eliminated by solving error distribution on gap direction of the joint-surface and the situation of the gap value.

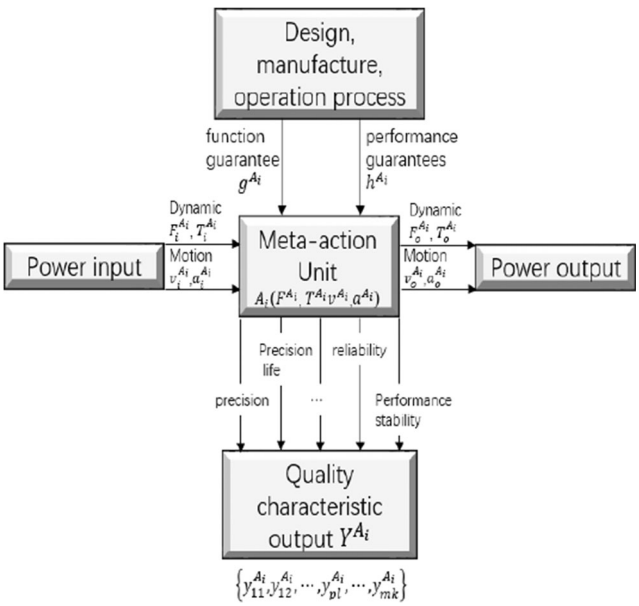

Fig. 2 Meta-action unit concept map

When the assembly is successful, the actual error transfer property of each joint-surface for the parallel joint-surfaces can be represented as follows:

$$\begin{aligned} A_{1R} &= A_{1S} \\ A_{2R} &= A_{2W} - A_{1S} \end{aligned} \tag{8}$$

Where the strong and the weak constraint of the parallel joint-surfaces are

$$\begin{aligned} A_S &= A_{1S} \\ A_W &= A_{2W} - A_{1S} \end{aligned} \tag{9}$$

Table 1 Joint-surface error transfer properties

Geometry of Joint-surface	Schematic diagram	Error transfer property
plane-plane	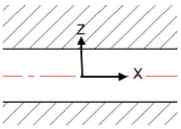	*α, β, w*
Plane-small Plane	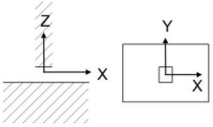	*w*
Plane-Narrow Plane	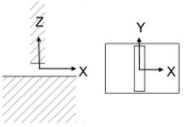	*α, w*
Plane Combination Surface-Plane Combination Surface	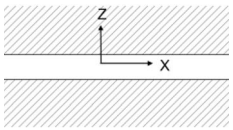	*α, β, w or β, w*
Cylinder-Cylinder	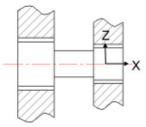	*α, β, μ, v*
Cylinder-Short Cylinder	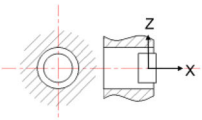	*μ, v*
Cylindrical Composite Surface-Cylindrical Composite Surface	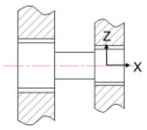	*α, β, μ, v*

(3) The parallel joint-surfaces are composed of two weak constraints. The intersection of the two combined surfaces is not empty. δ is the error component in the repeated constraint direction of parallel joint-surfaces. In the repeated constraint direction, the error component of the joint-surface 1 and 2 respectively are δ_1 and δ_2. When $\delta_1 < \delta_2$, assuming that joint-surface 1 transfers the error component of the parallel joint-surfaces, and entity interference is eliminated by adjusting the posture of weakly constrained direction of joint-surface 2.

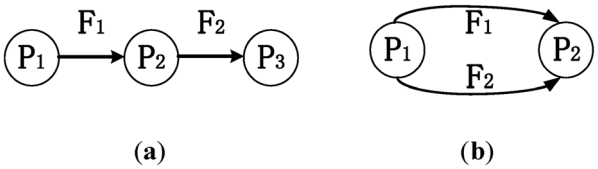

Fig. 3 Schematic diagram of serial-parallel joint-surfaces. **a**. Series connection. **b**. Parallel connection.

Assuming that the assembly is successful, and δ is transmitted by its joint-surface 1. The actual error transfer property of each joint-surface of the parallel joint-surfaces, is as follows:

$$\begin{aligned} A_{1R} &= A_{1W} \\ A_{2R} &= A_{2W} - A_{1W} \end{aligned} \tag{10}$$

The error transfer property of the parallel joint-surfaces is the set of the actual error transfer property of each composite joint-surface, such that

$$A = A_{1R} \cup A_{2R} \tag{11}$$

Where the error transfer property of the weak constraint for the parallel connection surface is

$$A_W = A_{1W} \cup (A_{2W} - A_{1W}) \tag{12}$$

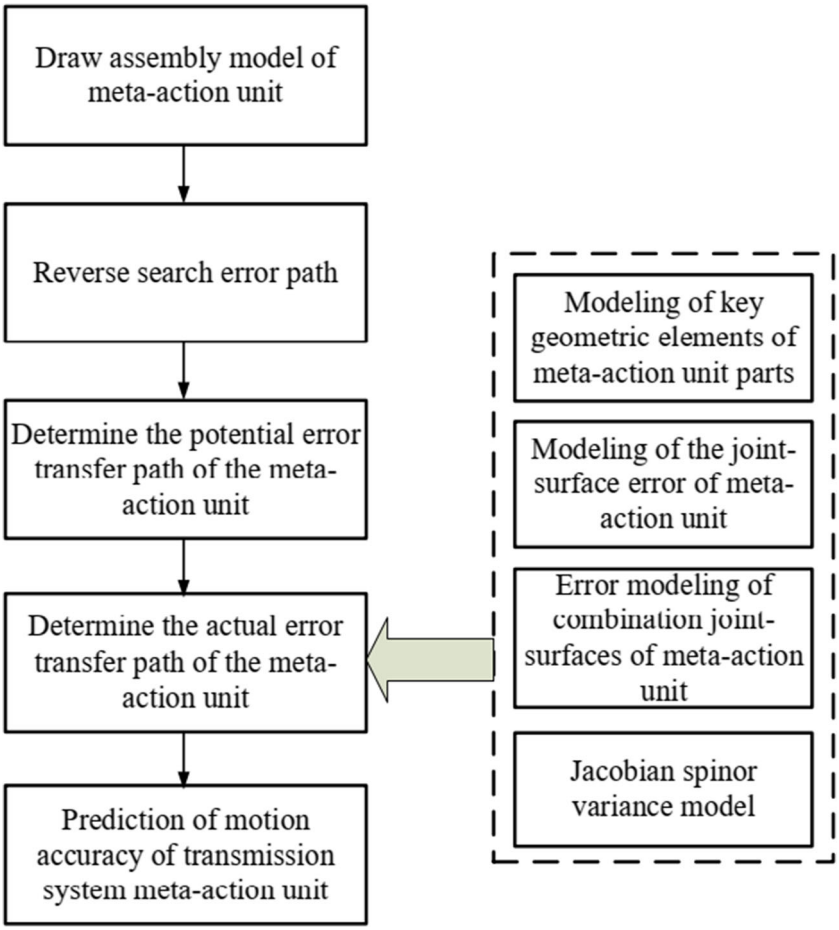

Fig. 4 Flow chart of the assembly precision prediction of the meta-action unit

The more the number of parallel joint-surfaces, the lower successful rate of assembly. In the process of product design, the number of parallel connection surfaces is usually less three.

4 Assembly precision prediction model of transmission system

The flow chart of the assembly precision prediction for the transmission system based on the machining error and the meta-action theory is shown in Fig. 4.

4.1 Analysis for error propagation paths

Determining the error transfer paths of the meta-action unit is an essential premise to establish the assembly error model, analyze the assembly error, and predict the precision of the meta-action unit. Therefore, we firstly established the assembly model of the meta-action unit through the structural analysis of the meta-action unit. Then, the error transfer paths were searched, and the potential error transfer paths were determined by qualitatively analyzing the error transfer property of the parallel connection joint-surface.

Meta-action unit assembly model is comprised of meta-action unit structure decomposition graph and meta-action unit assembly directed graph. Directed graph assembled describes the geometric structure information of meta-action unit by means of frame, circle, arc, dotted line, etc. It also called the error transfer paths and cannot only describe the geometric structure information, but also expresses the error transfer property between parts. Taking gear meta-action unit of the transmission system as an example, the structure decomposition diagram of gear meta-action unit and the directional diagram of the gear meta-action unit are shown in Figs. 5 and 6. In Fig. 6, if directed arc is a solid line, it means that the positioning constraint relation of two geometric elements is a strong constraint. Otherwise, it is a weak constraint. In the directed arc, error transmission property of the part's joint-surface represents the error transmission property among adjacent parts' joint-surfaces using 6 binary digits. For example, $B = (110001)$ represents the error components

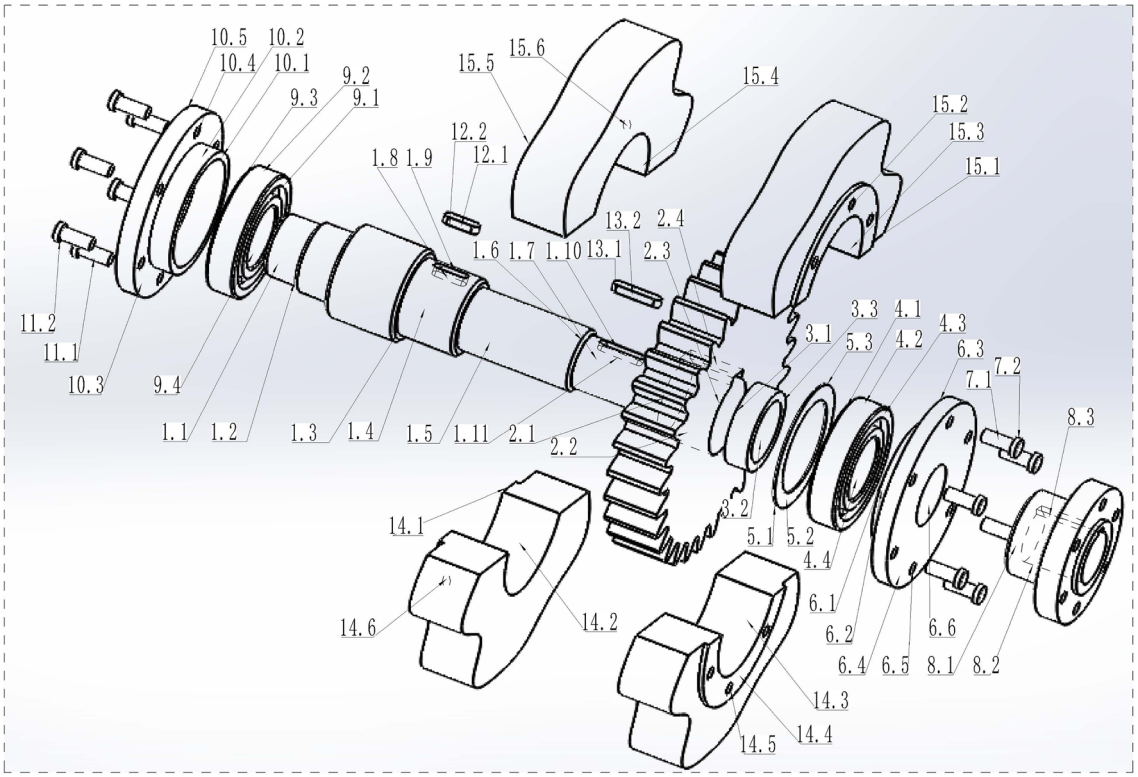

Fig. 5 Exploded view of the gear meta-action unit

of the bonding surface, α, β, and ω. The flowchart of the specific algorithm for searching error transfer paths is illustrated in Fig. 7.

Based on the assembly model of meta-action unit, the determining of error transfer paths is analyzed. The specific steps are as follows.

4.1.1 Determining the strut member and output member in meta-action unit and search the actual error transmission paths

The strut member and the output member of the meta-action unit are determined as the beginning and ends of the error

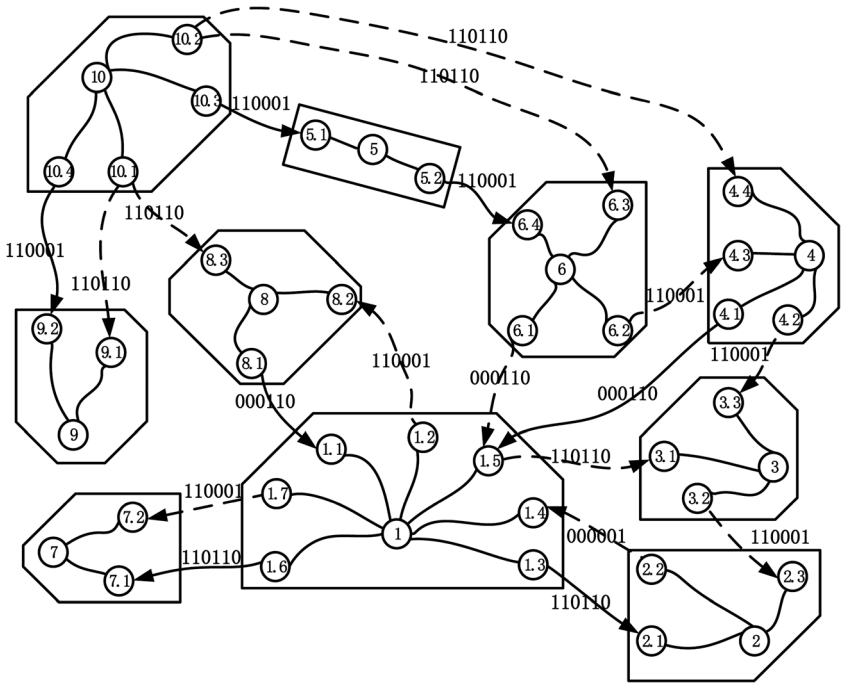

Fig. 6 Assembly directed graph of gear meta-action unit

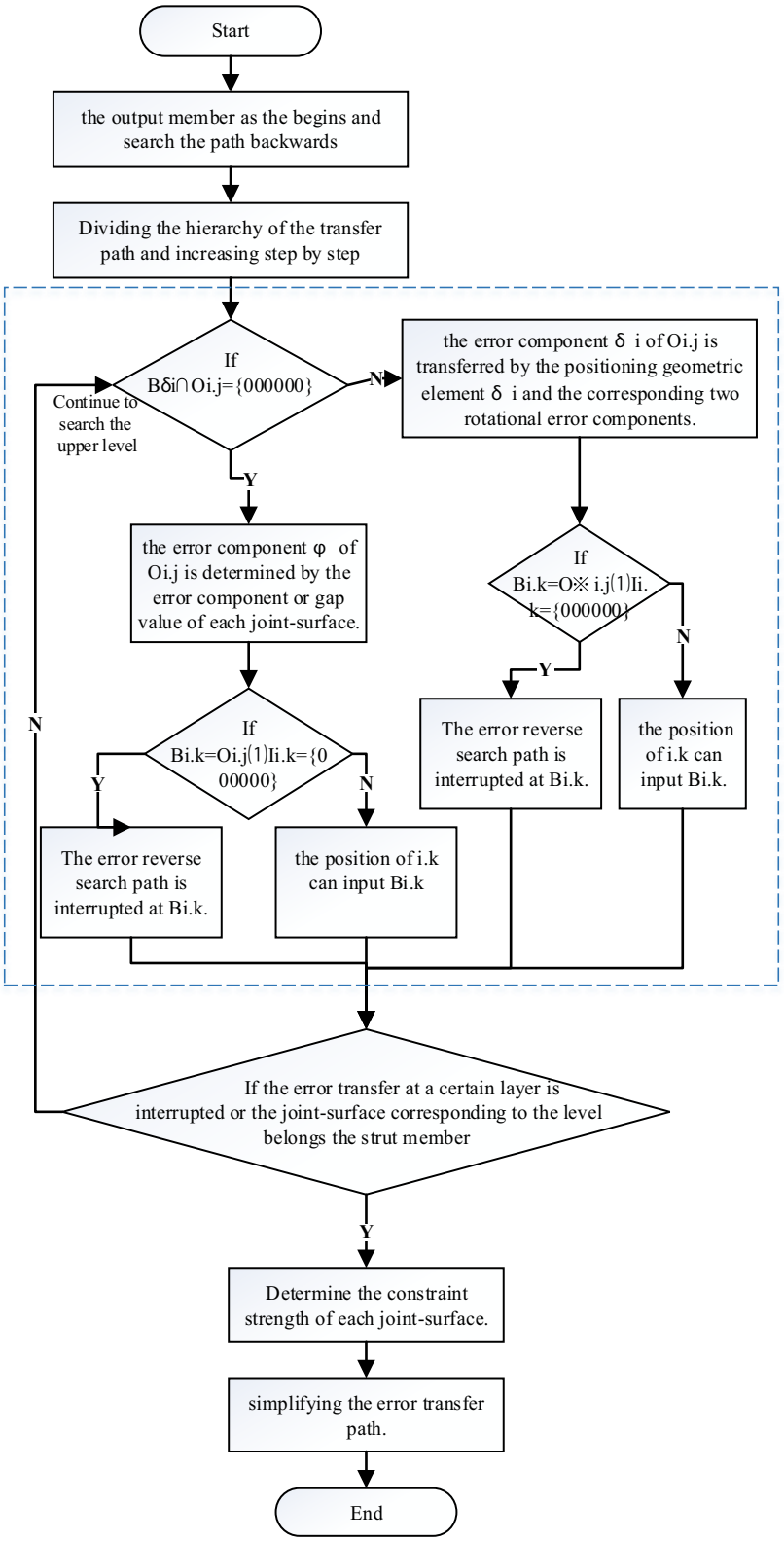

Fig. 7 The flowchart of the searching error transfer paths

transmission paths. According to the assembly model, the hierarchy of the transfer paths is divided into nodes of the joint-surface that is formed by the positioning geometric element and the positioned geometric element. According to the error transfer paths, the node of the output member is defined as level 1, and the hierarchy increases step by step with the joint-surface as the node. Taking gear meta-action unit as an example, the error reverse search paths is unfolded in a tree

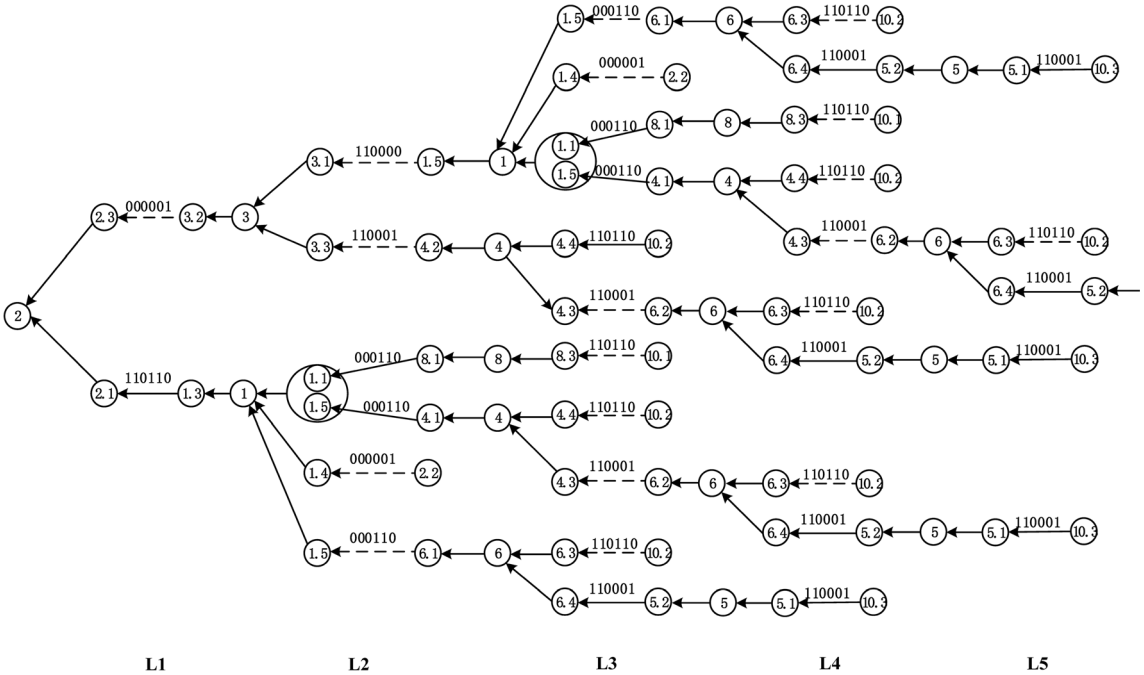

Fig. 8 Reverse search diagram of error paths in gear meta-action unit

structure. In Fig. 6, part 10 is used as a strut member and part 2 as an output member. The error reverse search paths are demonstrated in Fig. 8.

4.1.2 Determining the potential error transfer paths in meta-action unit

The potential error transfer paths are based on the error reverse search paths diagram. It starts from level 1. The error transfer property of each parallel joint-surfaces are qualitatively analyzed layer by layer. Afterwards, the error transfer interrupts paths are eliminated. It expresses the potential error components that can be transmitted to the output member of each joint-surface. The error transmission paths were simplified, and the foundation to obtain the actual error transmission paths were established. In the reverse search paths diagram of error, assuming that the geometric positioning elements *i, j* of parts *I* are at level 1, the output error component is $O_{i.\ j}$. And if the geometric positioned elements *i, k* are at level 1, the input error component is $I_{i.\ k}$. δ_i is the moving component in APW of part *I,* and $B_{\delta i}$ is expressed by 6 binary numbers. Then, the steps of the potential paths of error transfer are exhibited by the dashed box in the flowchart Fig. 7.

4.1.3 Determine the actual error transmission paths in meta-action unit

Based on the assembly model of meta-action unit, the reverse search paths of error in meta-action unit were obtained by searching the output member as the starting point. The potential error transfer paths were determined by qualitatively analyzing the error transfer property of the parallel joint-surfaces. Between the strut member and the output member, the potential output and input error components of each part were defined. For calculating the actual error transfer paths, firstly, the cumulative calculation of the potential error transfer paths was carried out through the Jacobian-Torsor variance model. Secondly, in the parallel error transfer level, the actual error transfer paths were determined by quantitatively analyzing the error transfer property of the parallel joint-surfaces layer by layer until the output member. Finally, the actual error transfer paths were determined.

4.2 Assembly precision prediction model

The demand of assembly precision index for the transmission system is the allowable range of the maximum error, which is geometric elements in the specified direction during the movement of the output member. We can define that the assembly precision index of the gear meta-action unit acts on the rotary axis of output member. And the assembly precision index of the moving meta-action unit is decided by the moving axis of output member. So based on the Jacobian-Torsor model, the error components on the actual error transfer paths were calculated cumulatively. Finally, we can obtain the distribution of the error components of the output member. In the gear meta-action unit, the radial displacement error component $u \sim N(u(\theta), \sigma_u)$, $v \sim N(v(\theta), \sigma_v)$, radial rotational error component $\alpha \sim N(\alpha(\theta), \sigma_\alpha)$, $\beta \sim N(\alpha(\theta), \sigma_\beta)$, and axial shifting error component $w \sim N(w(\theta), \sigma_v)$ are independent on each other.

$E_{r1}(\theta) = t = \sqrt{u(\theta)^2 + v(\theta)^2}$, $E_{r2}(\theta) = r = \sqrt{\alpha(\theta)^2 + \beta(\theta)^2}$, and $E_{r3}(\theta) = c = w(\theta)$ can be obtained. Then, E_{r1} and E_{r2} follow Rayleigh distribution and E_{r3} follow normal distribution. Their probability density distribution function is shown in formula (13):

$$\begin{cases} f(t) = \dfrac{t - E_{r1}(\theta)}{1.02e^{-5}} e^{-\frac{(t-E_{r1}(\theta))^2}{2\times 1.02e-05}} (t > 0) \\ f(r) = \dfrac{r - E_{r2}(\theta)}{9.6e^{-9}} e^{-\frac{(r-E_{r2}(\theta))^2}{2\times 9.6e-09}} (r > 0) \\ f(c) = \dfrac{1}{\sqrt{2\pi} \times 0.0072} e^{-\frac{(c-E_{r3}(\theta))^2}{2\times 0.0072}} \end{cases} \tag{13}$$

Assuming that the maximum allowable error range of precision indexes of radial movement, radial rotation and axial shifting are Ω_t, Ω_r and Ω_c respectively. Then the integral is the distribution density function of the assembly precision index on Ω, and it can solve the assembly precision reliability of the meta-action unit. Precision reliability is the probability that the expected error value of the mechanical parts falls within the maximum allowable error range of the assembly. In this paper, the assembly precision reliability of meta-action unit is defined as the probability of the maximum allowable error range where the expected precision value of the output in assembly meta-action unit locates. $R(x)$ represents the reliability, and the specific expression is as follows:

$$R(x) = \int_{\Omega_t/2} f(t)dt \times \int_{\Omega_r/2} f(r)dr \times \int_{\Omega_c/2} f(c)dc \tag{14}$$

Similarly, the reliability calculation of assembly precision for moving meta-action unit is similar to that of rotating meta-action unit. Machining error and the error caused by positioning operation in assembly are the motion error of meta-action unit. In the assembly process, the errors can be controlled by changing the assembly process, so it can be ignored temporarily.

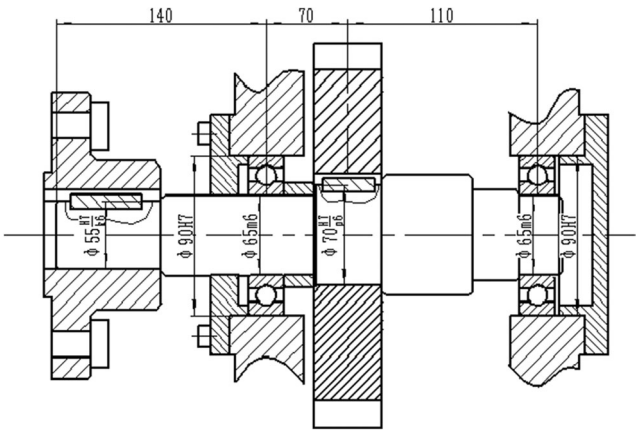

Fig. 9 Gear meta-action unit

5 Application

In this section, taking the analysis of NC machining center's subsystem of an enterprise as an example, based on geometric error modeling of parts, the process and idea of assembly precision prediction method are elaborated in detail. The feasibility of this method is demonstrated. Figure 9 is the meta-action unit of the gear and the key components are gears, couplings, rolling bearings, shafts, bushes, gaskets, bearing end caps, sealing rings, and boxes. The precision design of key geometric elements is displayed in Fig. 10. Assuming that the assembly error caused by positioning operation is not considered. In order to ensure the assembly precision of the gear transmission, the radial displacement error $E_{r1} \le 0.04$, the radial rotation error $E_{r2} \le 0.002$, the axial shifting error $E_{r3} \le 0.4$ is required, and the reliability is 98%.

5.1 Assembly precision prediction of gear meta-action unit

Here, according to the flowchart in Fig. 4, we predicted the assembly precision of rotation meta-action unit in the gear transmission system. Firstly, we drew the assembly model of the gear meta-action unit based on the assembly model of the gear meta-action unit, as shown in Figs. 5 and 6. Secondly, according to the error transfer paths of the assembly model, we searched error transfer paths reversely, as shown in Fig. 8. Then, we ascertained error transfer paths of meta-action unit and predicted assembly precision, as shown below:

5.1.1 Determination of error transfer paths in meta-action unit

Potential error transfer paths In Fig. 8, the positioning geometric element 3.2 of part 3 is at level 1, and the output-error component is $O_{3.2} = \{110001\}$. The positioned geometric element 3.1 is at level 2, and the input-error component is $I_{3.1} = \{110110\}$. The plane non-cling fit's displacement error component of part 3 under clearance direction is $B_{\delta 3} = \{000001\}$, and $B_{\delta 3} \cap O_{3.2} \neq \{000000\}$. Then the auxiliary output error component $\overline{O}_{3.2} = B'_{\delta 3} \cup O_{3.2} = \{110000\} \cup \{110001\} = \{110001\}$ was needed to be calculated. At this point, $B_{3.1} = \overline{O}_{3.2} \cap I_{3.1} = \{110000\}$ represents that the error component in the direction of $\{110000\}$ can be input at 3.1. Continuing to search the upper level, the positioned geometric element 3.1 of part 3 fits with the positioning geometric element 1.5 of part 1. The positioned geometric element of part 1 is the combined surface 1.1-1.5 at level. The plane non-cling fit's displacement error component of part 3 under clearance direction is $B_{\sigma 1} = \{000001\}$, and $B_{\sigma 1} \cap B_{3.1} = \{000000\}$. At this point, $B_{1.1-1.5} = B_{3.1} \cap I_{1.1-1.5} = \{110000\} \cap \{110110\} = \{110000\}$ represents that the error component in the direction of $\{110000\}$

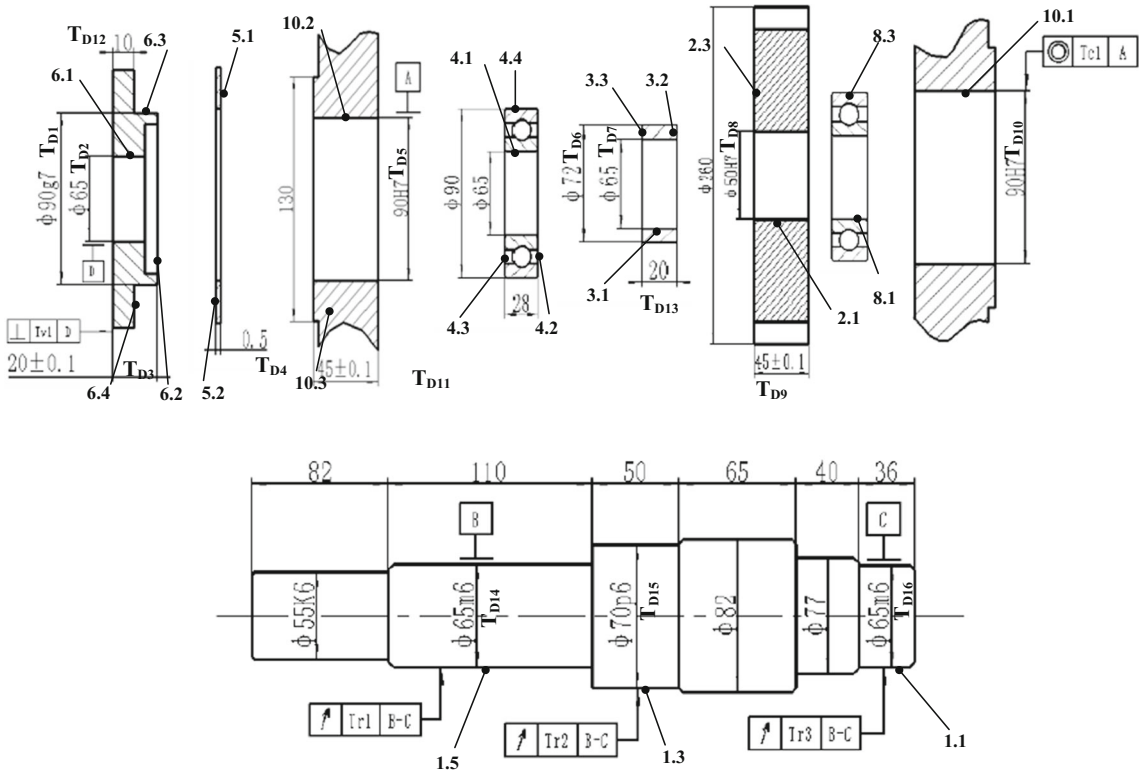

Fig. 10 Geometric element of the gear meta-action unit

can be put at composite joint-surface 1.1–1.5. Then the upper level was searched continuously until that the error transfer is interrupted or the joint-surface corresponding to the level belongs to the supporting member. The parts are usually positioned by multiple geometric elements, so it is necessary to analyze the paths. The paths are where positioned geometric element 3.3 of part 3 at level 1 and positioned geometric element 1.3 and 1.4 of part 1 at level 2. Finally, the error transmission paths can be further simplified by determining the constraint strength of each joint-surface, and then the potential error transfer paths of gear meta-action unit can be obtained, as shown in Fig. 11.

Actual error transfer paths There are four parallel joint-surfaces in the potential error transfer paths of gear meta-action unit : $F_{3-(F3-F8)}$, $F_{2-(F9-F10)}$, $F_{2-(F67-F11)}$, and $F_{1-(F12-F13)}$. $F_{1-(F12-F13)}$ is the parallel joint-surfaces which is composed by F_i and F_j at the level n of potential error transfer paths. Jacobian-Torsor variance model analyzed quantitatively the actual error transfer paths of each parallel joint-surface. The details are shown in Tables 2 and 3. Firstly, the error transfer property of $F_{3-(F3-F8)}$ in parallel connection is analyzed as an example.

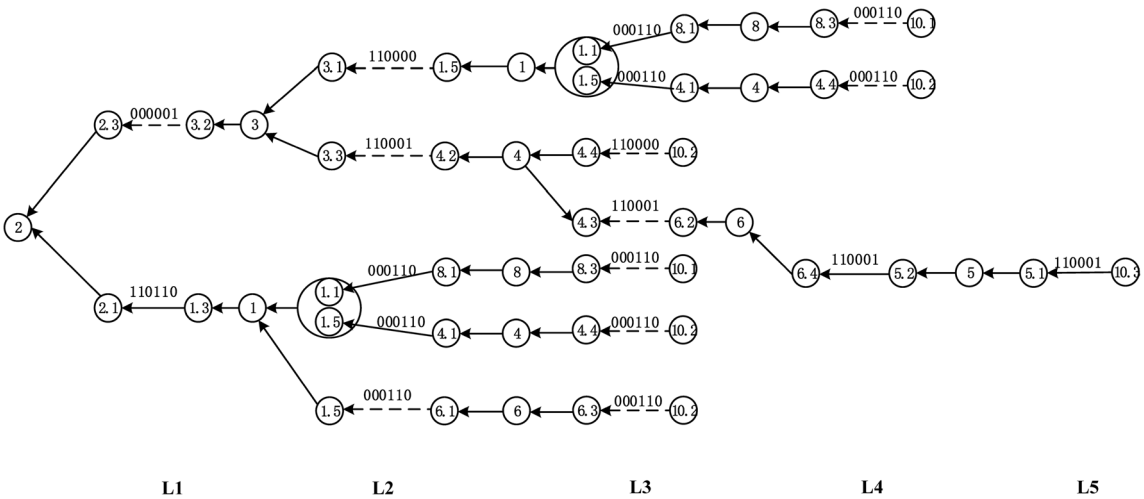

Fig. 11 Potential error transfer paths of the gear meta-action unit

Table 2 Joint-surface and tolerance term of potential error transfer in gear meta-action unit

Joint-surface (symbol)	Clearance value TS	Geometric elements	Relevant tolerances	Tolerance range
Planar adjacent JS	——	Plane 10.3	Dimensional tolerance TD11	[− 0.2, 0.2]
10.3–5.1 (F1)		Plane 5.1	Datum geometric elements	——
Cylindrical gap JS	0.028	Cylinder 10.1	Dimensional tolerance TD10	[0, 0.035]
10.1–8.3 (F2)			Coaxiality tolerance TC1	0.01
		Cylinder 8.3	Dimensional tolerance neglected	——
Cylindrical gap JS	0.028	Cylinder 10.2	Dimensional tolerance TD5	[0, 0.035]
10.2–4.4 (F3)		Cylinder 4.4	Dimensional tolerance neglected	0
Cylindrical gap JS	0.041	Cylinder 10.2	Dimensional tolerance TD5	[0, 0.035]
10.2–6.3 (F4)		Cylinder 6.3	Dimensional tolerance TD1	[− 0.047, − 0.012]
Planar adjacent JS	——	plane5.2	Dimensional tolerance TD4	− 0.1,0.1]
5.2–6.4 (F5)		plane6.4	Dimensional tolerance TD12	[− 0.2,0.2]
Cylindrical interference JS	——	Cylinder 8.1	Dimensional tolerance neglected	——
8.1–1.1 (F6)		Cylinder 1.1	Dimensional tolerance T_{D16}	[0.011, 0.030]
			Circular run-out error T_{R3}	0.01
Cylindrical interference JS	——	Cylinder 4.1	Dimensional tolerance neglected	——
4.1–1.5 (F7)		Cylinder 1.5	Dimensional tolerance T_{D14}	[0.011, 0.030]
			Circular run-out error T_{R1}	0.01
Planar non-compact JS	——	plane6.2	Dimensional tolerance T_{D3}	[− 0.2,0.2]
6.2–4.3 (F8)			Perpendicularity T_{V1}	0.02
		plane4.3	Dimensional tolerance neglected	——
Cylindrical gap JS	0.2	Cylinder 1.5	Dimensional tolerance T_{D14}	[0.011, 0.030]
1.5–3.1 (F9)			Circular run-out error T_{R1}	0.01
		Cylinder 3.1	Dimensional tolerance T_{D7}	[− 0.3,0.3]
Planar non-compact JS	——	plane4.2	Dimensional tolerance neglected	——
4.2–3.3 (F10)		plane3.3	Datum geometric elements	——
Cylindrical gap JS	0.1	Cylinder 6.1	Dimensional tolerance T_{D2}	[− 0.2,0.2]
6.1–1.5 (F11)		Cylinder 1.5	Dimensional tolerance T_{D14}	[0.011, 0.030]
			Circular run-out error T_{R1}	0.01
Planar non-compact JS	——	plane3.2	Dimensional tolerance T_{D13}	[− 0.2,0.2]
3.2–2.3 (F12)		plane2.3	Dimensional tolerance T_{D9}	[− 0.1,0.1]
Cylindrical interference JS	——	Cylinder 1.3	Dimensional tolerance T_{D15}	[0.032, 0.051]
1.3–2.1 (F13)			Circular run-out error T_{R2}	0.015
		Cylinder 2.1	Dimensional tolerance T_{D8}	[0, 0.025]

1) Establishment of an error model for parallel joint-surface $F_{3-(F3-F8)}$.

$$FR_{3-F3} = \left[0, 0, 0, \sigma^2_{\alpha 3}, \sigma^2_{\beta 3}, 0\right]^T \tag{15}$$

WhereFR_{n-Fi} is the cumulative transfer error of joint-surface i at the potential error transfer paths level n.

2) Solving the variance of geometric elements that are related to parallel joint-surfaces. After calculation:

$$\begin{cases} \sigma^2_{\alpha 3-F3} = \sigma^2_{\alpha 3} = 3.6e^{-8} \\ \sigma^2_{\beta 3-F3} = \sigma^2_{\beta 3} = 3.6e^{-8} \\ \sigma^2_{w3-F8} = \sigma^2_{w1} + \sigma^2_{w5} + \sigma^2_{w8} = 0.0061 \\ \sigma^2_{\alpha 3-F8} = \sigma^2_{\alpha 1} + \sigma^2_{\alpha 5} + \sigma^2_{\alpha 8} = 4.9e^{-7} \\ \sigma^2_{\beta 3-F8} = \sigma^2_{\beta 1} + \sigma^2_{\beta 5} + \sigma^2_{\beta 8} = 4.9e^{-7} \end{cases} \tag{16}$$

3) Solving the error transfer property analysis of parallel joint-surfaces. Because$A_{3S} \cap A_{8s} = \phi$, $(A_{3s} \cup A_{8s}) \cap (A_{3W} \cup A_{8W}) = \phi$ and $\delta = A_{3W} \cap A_{8W} \neq \phi$ are known. From$\sigma_{\alpha 3-F3} < \sigma_{\alpha 3-F8}$ and $\sigma_{\beta 3-F3} < \sigma_{\beta 3-F8}$, it can be assumed that joint surface F_3 transfer the error component of the parallel joint surface. The interference can be eliminated by calculating the error distribution in the gap direction of the joint surface, so the hypothesis is correct. The error component distribution of parallel joint surface is calculated:

$$\begin{aligned} \sigma^2{}_{\alpha 3-(F3-F8)} &= \sigma^2{}_{\alpha 3-F3} = 3.6e^{-0.8} \\ \sigma^2{}_{\beta 3-(F3-F8)} &= \sigma^2{}_{\beta 3-F3} = 3.6e^{-0.8} \end{aligned} \tag{17}$$

Where $w \notin \delta$, $W \in A_{sw}$, $\delta_w \in A_{pw}$.

So, w takes the minimum value without interference as follows. The mean value of each error component of $F_{3-(F3-F8)}$ in parallel joint is 0.

Table 3 Potential error transfer properties and assembly location information of each joint-surface

Joint Surface	Actual error transfer property		Locating origin of characteristic coordinates
	Strong constraints	Weak constraints	
F1	α, β, w	——	(0,0,116.5)
F2	——	u, v	(0,0,320)
F3	——	u, v	(0,0,140)
F4	——	α, β	(0,0,121)
F5	α, β, w	——	(0,0,116)
F6	——	u, v	(0,0,320)
F7	——	u, v	(0,0,140)
F8	——	α, β, w	(0,0,126)
F9	——	α, β	(0,0,164)
F10	——	α, β, w	(0,0,154)
F11	——	u, v	(0,0,113.5)
F12	——	w	(0,0,174)
F13	——	α, β, u, v	(0,0,210)

$$\sigma^2_{w_{3-(F_3-F_8)}} = 0.0104 \tag{18}$$

In the same way, we analyzed the error transfer properties of $F_{2-(F_9-F_{10})}$, $F_{2-(F_{67}-F_{11})}$, and $F_{1-(F_{12}-F_{13})}$. The error component α and β of the parallel joint-surfaces $F_{2-(F_9-F_{10})}$ are transmitted by joint-surface F_{10}. The error component u,and v of the parallel joint-surface $F_{2-(F_{67}-F_{11})}$ are transmitted by joint-surface F_{67}. The parallel joint-surface $F_{1-(F_{12}-F_{13})}$ is composed of two weak parallel joint-surfaces that are no intersection, so the corresponding joint-surface transmitted the error components of the parallel joint-surface. In summary, error transfer properties of parallel joint-surfaces are quantitatively analyzed by Jacobian-Torsor variance model, and then the actual error transfer paths of gear element action unit were obtained, as shown in Fig. 12.

5.1.2 Prediction of assembly precision

Prediction of each error component value for gear meta-action unit The variance of each error component for the output member was as follows:

$$\begin{cases} \sigma_u^2 = \sigma^2_{u_1-(F_{12}-F_{13})} = 1.02e^{-5} \\ \sigma_v^2 = \sigma^2_{v_1-(F_{12}-F_{13})} = 1.02e^{-5} \\ \sigma_\alpha^2 = \sigma^2_{\alpha_1-(F_{12}-F_{13})} = 9.6e^{-9} \\ \sigma_\beta^2 = \sigma^2_{\beta_1-(F_{12}-F_{13})} = 9.6e^{-9} \\ \sigma_w^2 = \sigma^2_{w1-(F_{12}-F_{13})} = 0.0072 \end{cases} \tag{19}$$

The mean value of the error components for the output member was as follows:

$$\begin{cases} \mu_\alpha = \mu_{\alpha 67} = \dfrac{\cos\theta\sqrt{25\cos^2\theta + 16\sin^2\theta} - \cos(\theta+\varphi)\sqrt{25\cos^2(\theta+\varphi) + +16\sin^2(\theta+\varphi)}}{1.8\times 10^8} \\ \mu_\beta = \mu_{\beta 67} = \dfrac{\sin\theta\sqrt{25\cos^2\theta + 16\sin^2\theta} - \sin(\theta+\varphi)\sqrt{25\cos^2(\theta+\varphi) + 16\sin^2(\theta+\varphi)}}{1.8\times 10^8} \\ \mu_u = \mu_{u67} = \dfrac{7}{1.8\times 10^7}\sin\theta\sqrt{25\cos^2\theta + 16\sin^2\theta} + \dfrac{11}{1.8\times 10^7}\sin(\theta+\varphi)\sqrt{25\cos^2(\theta+\varphi) + 16\sin^2(\theta+\varphi)} \\ \mu_v = \mu_{v67} = \dfrac{7}{1.8\times 10^7}\cos\theta\sqrt{25\cos^2\theta + 16\sin^2\theta} + \dfrac{11}{1.8\times 10^7}\cos(\theta+\varphi)\sqrt{25\cos^2(\theta+\varphi) + 16\sin^2(\theta+\varphi)} \\ \mu_w = \mu_{w10} = \left(8e^{-6}\right)\sin\theta \end{cases} \tag{20}$$

Reliability solution for assembly precision of gear meta-action unit First, the probability density of assembly precision index is calculated. The radial displacement error component are $u \sim N(\mu_u(\theta), 1.02e^{-5})$ and $\sim N(\mu_v(\theta), 1.02e^{-5})$. Radial rotational error component are $\alpha \sim N(\mu_\alpha(\theta), 9.6e^{-9})$ and $\sim N(\mu_\beta(\theta),$

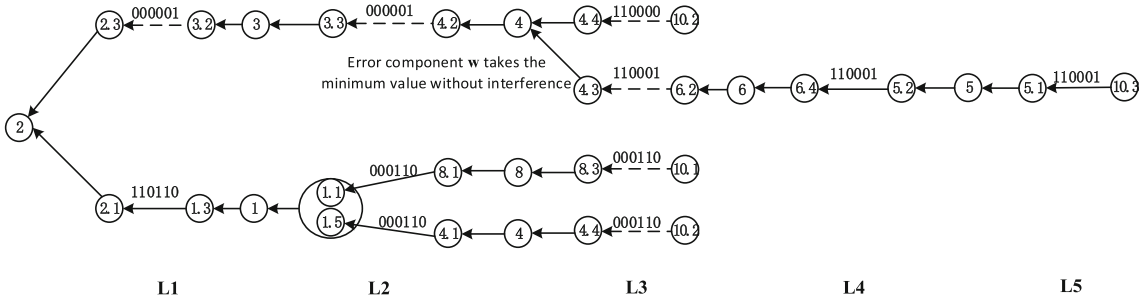

Fig. 12 Actual error transfer paths of the gear meta-action unit

$9.6e^{-9}$). Axial shifting error component is ~$N(\mu_w(\theta), 0.0072)$. And each error component is independent of each other. $E_{r1}(\theta) = t = \sqrt{u(\theta)^2 + v(\theta)^2}$, $E_{r2}(\theta) = r = \sqrt{\alpha(\theta)^2 + \beta(\theta)^2}$ and $E_{r3}(\theta) = c = w(\theta)$ can be got. Then E_{r1} and E_{r2} obey Rayleigh distribution and E_{r3} obeys normal distribution. Their probability density distribution functions are expressed by the formula (21):

$$\begin{cases} f(t) = \dfrac{t - E_{r1}(\theta)}{1.02e^{-5}} e^{-\frac{(t-E_{r1}(\theta))^2}{2\times 1.02e^{-5}}} (t > 0) \\ f(r) = \dfrac{r - E_{r2}(\theta)}{9.6e^{-9}} e^{-\frac{(r-E_{r2}(\theta))^2}{2\times 9.6e^{-9}}} (r > 0) \\ f(c) = \dfrac{1}{\sqrt{2\pi}\times 0.0072} e^{-\frac{(c-E_{r3}(\theta))^2}{2\times 0.0072}} \end{cases} \tag{21}$$

Probability density distributions of E_{r1}, E_{r2}, and E_{r3} are shown in Fig. 13.

Second, reliability solutions are calculated. Gear axis requirements are listed below: radial displacement error $E_{r1} \leq 0.04$, radial rotation error $E_{r2} \leq 0.002$, and axial shifting error $E_{r3} \leq 0.4$. Then, the assembly precision reliability of the gear meta-action unit is expressed as follows:

$$\begin{aligned} R(x) &= \int_{\Omega_{t/2}} f(t)\, dt \times \int_{\Omega_{r/2}} f(r)\, dr \times \int_{\Omega_{c/2}} f(c) \\ dc &= \int_0^{0.02} \frac{t - E_{r1}(\theta)}{\sigma_u^2} e^{-\frac{(t-E_{r1}(\theta))^2}{2\sigma_u^2}} dt \times \int_0^{0.001} \frac{r - E_{r2}(\theta)}{\sigma_\alpha^2} e^{-\frac{(r-E_{r2}(\theta))^2}{2\sigma_\alpha^2}} \\ dr &\times \int_{-0.2}^{0.2} \frac{1}{\sqrt{2\pi}\sigma_w} e^{-\frac{(c-E_{r3}(\theta))^2}{2\sigma_w^2}} dw \end{aligned} \tag{22}$$

Where, in terms of the diameter value of the minimum enveloping circle is the corresponding index of the error value principle. $E_{r1}(\theta)$, $E_{r2}(\theta)$, and can take the diameter value of their smallest enveloping circle in polar coordinates, so the calculated value of reliability is more conservative. By calculating, the diameters of the minimum enveloping circle of $E_{r1}(\theta)$, $E_{r2}(\theta)$, and $E_{r3}(\theta)$ in polar coordinates are $E_{r1} = 5e^{-6}$, $E_{r2} = 7.9e^{-9}$, and $E_{r3} = 4e^{-6}$ respectively. Substituting them and the following formulas are calculated.

$$R(t) = R(E_{r1}) \times R(E_{r2}) \times R(E_{r3}) = 0.9815 \tag{23}$$

The reliability of assembly precision for the gear meta-action unit is 98.2%; therefore, the assembly precision meets the requirement.

5.2 Validation

5.2.1 Measurement and simulation

According to the measurement precision of the gear meta-action unit, the gear axis precision of the meta-action assembly unit was measured by a double-sided meshing comprehensive precision measuring instrument as shown in Fig. 14. We got 30 sets of the measured data: the radial integrated error $E_{rz}(\theta) = \sqrt{E_{r1}^2 + E_{r2}^2}$, and the axial shifting error $E_{r3}(\theta)$. Precision reliability of the gear meta-action unit was obtained. The part of measurement data is displayed in Table 4 below:

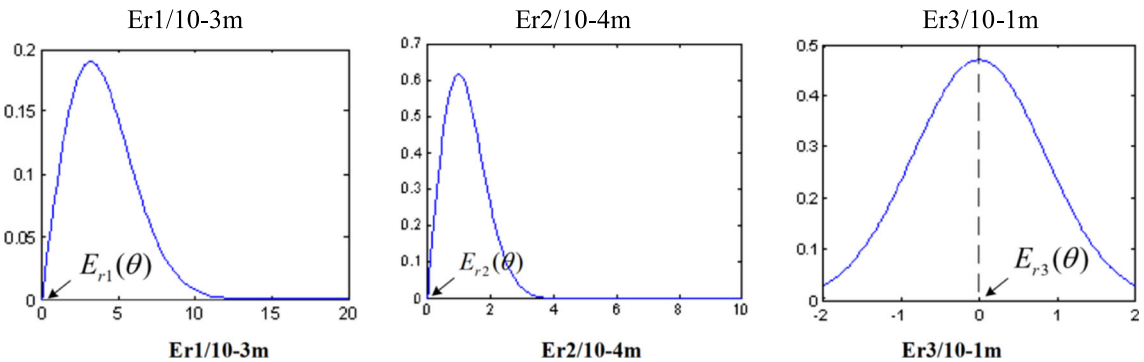

Fig. 13 Assembly precision index distribution

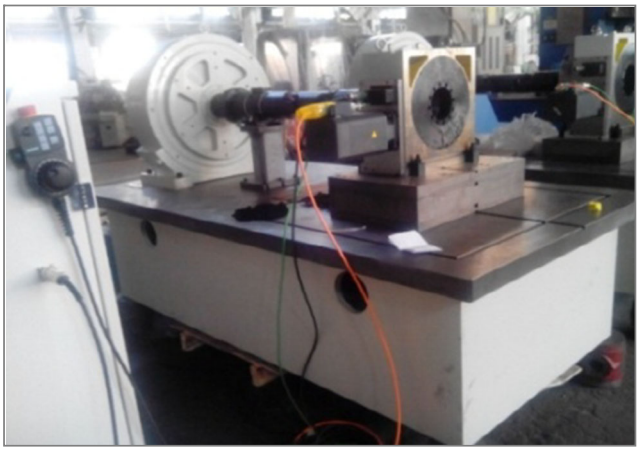

Fig. 14 The scene photo of the assembly gear meta-action unit

The predicted theoretical data:

$$E_{rz}(\theta) = \sqrt{E_{r1}^2 + E_{r2}^2} = 0.012394 = 4.997e^{-6}/10^{-3}m \quad E_{r3}(\theta) = 4.000e^{-6}/10^{-3}m \tag{24}$$

The measured average data:

$$\overline{E'_{rz}}(\theta) = \frac{\sum_{i=1}^{n} E'_{rzi}}{n} 4.823e^{-6}/10^{-3}m \quad , \quad \overline{E'_{r3}}(\theta) = 3.910e^{-6}/10^{-3}m \tag{25}$$

As this batch of machine tools accessories is produced in small batches, Monte Carlo (MCS) simulation method was adopted to contrast the predictive reliability value. As one of the important methods of system reliability measurement, when the model is unknown, MCS simulation can accurately solve the model reliability [32]. CATIA was used to establish 3D assembly model for simulation analysis. And then the parameter setting method was used to simulate assembly model of gear meta-action unit. The radial and axial position change curves of gear axis were output. After that, we monitored the change curves to analyze if the output precision of assembly meta- action unit complies with the requirements. In order to verify the feasibility of the above theoretical method, Monte Carlo method was adopted for the comparative verification experiment. The calculation formula of reliability is as formula (26). Finally, the actual precision reliability value of gear meta-action unit was obtained through calculating the average value of multiple assembly precision reliability.

$$R = \frac{N_f}{N_t} \tag{26}$$

Where N_t is the total times of simulation, $N_f$is the sum of simulation times of $E_{r1} \le 0.04$ $E_{r2} \le 0.04$, and $E_{r3} \le 0.04$.

The assembly gear meta-action unit was simulated for 10*4 times. The precision reliability value was calculated once every 100 times by setting program. Then, the data was output in the form of a line graph.

As shown in Fig. 15, with the number of simulation experiments increases, the calculated value of precision reliability tended to a certain stable value. When the number of experiments reached over 5000 times, the calculated result of precision reliability converged to around 0.985, so the obtained precision reliability obtained by the Monte Carlo method was 0.985. The result proved that the theoretical value is slightly less than the actual value of simulation, because the values of $E_{r1}(\theta)$, $E_{r2}(\theta)$, and $E_{r3}(\theta)$ that we chose are the diameters of their minimum enveloping circles in polar

Table 4 The measured value of gear axis precision in assembly meta-action unit

	$E'_{rz}(\theta)/10^{-3}$ m	$E'_{r3}(\theta)/10^{-3}$ m		$E'_{rz}(\theta)/10^{-3}$ m	$E'_{r3}(\theta)/10^{-3}$ m
1	4.936	3.163	16	4.673	3.031
2	5.012	4.025	17	4.789	3.589
3	3.689	3.156	18	4.476	3.968
4	4.187	2.986	19	4.910	3.741
5	4.568	4.532	20	5.257	4.252
6	4.596	3.150	21	4.810	4.375
7	5.110	4.271	22	4.694	3.489
8	4.963	3.785	23	4.763	4.405
9	4.981	4.168	24	5.176	3.245
10	5.203	3.786	25	4.893	3.587
11	4.752	3.414	26	5.157	4.841
12	4.952	4.234	27	4.478	3.910
13	5.114	4.781	28	4.695	3.369
14	5.237	5.314	29	4.760	4.027
15	4.856	4.611	30	5.003	4.122

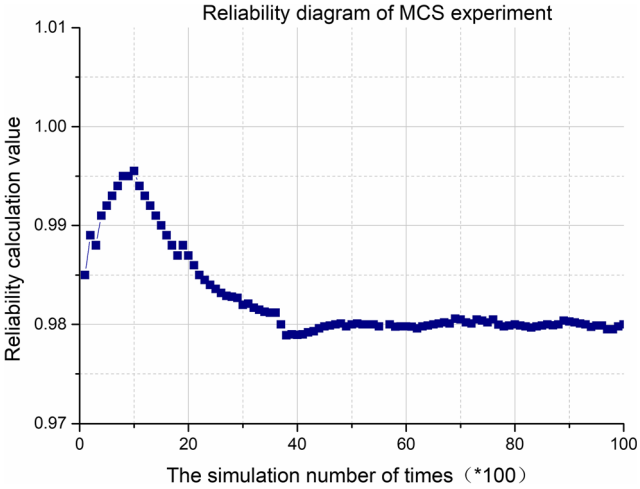

Fig. 15 Precision reliability of gear meta-action unit under MCS experiment

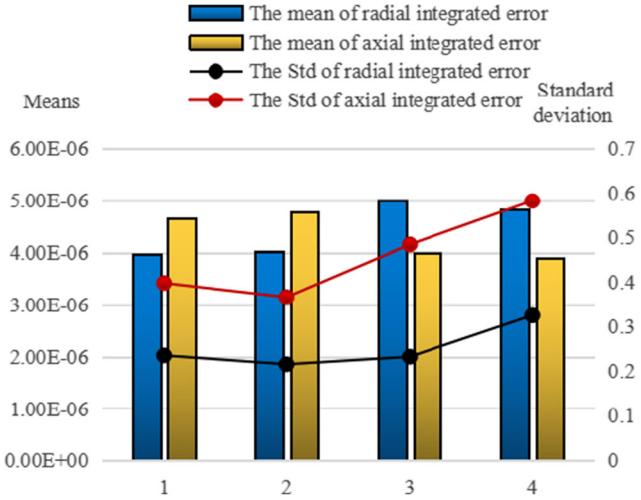

Fig. 16 Results of different method and actual value comparison

coordinates. So the prediction precision and reliability value are more conservative. The design requires that the precision reliability of the gear axis of the meta-action unit should be more than 98%. Both the theoretical predicted value and the results obtained by Monte Carlo simulation meet the design requirements, and the error of the results is less than 1%. We can know that the precision prediction method is feasible. Therefore, we explored an intuitive new theoretical method to predict the objective level of design precision and verified this method.

6 Comparison and discussion

In this part, to further verify the effectiveness of the proposed prediction method for assembly precision of transmission system, a comparison analysis with other existing traditional methods such as the dimensional chain method(DC), the unified Jacobian-Torsor model (UJT) are taken into consideration. Table 5 demonstrates the results' comparisons of means and standard deviations using different prediction approaches and actual values. Based on the information in Table 5, the four results' trends of means and standard deviations for radial integrated error and axial movement error are displayed in Fig. 16.

Table 5 lists four results of means and standard deviations. Among them, the dimensional chain method is a traditional and mature method. The unified Jacobian-Torsor model was introduced in cited above. From Fig. 16, the comparison of the four results can be intuitively seen from Fig. 16. The mean value (3) is higher than the mean value (4) of about 3.67%, while the mean value (1) is lower than the (4) of about 17.83%, which illustrates that the means of the radial integrated error and the axial shifting error obtained from the proposed method is closer to the actual value than other two mature model. The standard deviation of actual value is slightly higher than other prediction method, which is because of the assembly process, assembly environment, personnel technology, etc. The standard deviation (2) of the radial and axial error are respectively lower than (4) of about 33.67% and 36.95%, and it does not match the actual situation relatively. The standard deviations (3) are lower than the actual value of about 28.48% and 16.8%. It confirms that the results of the radial integrated error and the axial shifting error of the proposed method are closer to the actual values, it is because the proposed method proposed takes into account the positioning relationship and the strength relationship of constraints among each joint-surface of part in the unit during the process of

Table 5 Results of experiment and three methods

Order	Method	The radial integrated error/*mm*		The axial shifting error/*mm*	
		Mean	Standard deviation	Mean	Standard deviation
1	Unified Jacobian-Torsor model	3.963e−6	0.2357	4.673e−6	0.3989
2	Dimensional chain method	4.025e−6	0.2159	4.789e−6	0.3674
3	The proposed method	4.997e−6	0.2328	4.00e−6	0.4848
4	The actual value	4.823e−6	0.3255	3.910e−6	0.5827

qualitatively and quantitatively searching for error paths. So its fluctuation is relatively more in line with the actual value.

The comparisons above show that the proposed method is more suitable and effective for predicting precision of the mechanical system and can provide a basis for designers to make and optimize design scheme effectively.

7 Conclusions

(1) Under multi-tolerance coupling, the proposed geometric element error modeling method deduced the actual distribution law of each error component parameter using the unqualified rate P of the constraint equation. The geometric element error model of the transmission system is established.

(2) It is qualitatively analyzed that the joint-surface's error transfer mechanism of the parts in the unit, and the error transfer properties among the joint-surfaces of the adjacent parts are represented by 6-bit binary numbers. A method for searching the cumulative transfer paths of potential errors in the transmission system was proposed.

Then, in order to find the actual error transfer paths at the parallel error transfer level, and analyze layer-by-layer until determining the actual error cumulative transfer paths of the meta-action unit in the transmission system, there is a quantitative analysis of the error transfer properties. Finally, the motion precision prediction model of the transmission system is established by combining Jacobian-Torsor method.

(3) Reliability is proposed as the basis to evaluate the performance of the motion precision, so it can be used to evaluate the ability of assembly to meet the precision requirements, which is more in line with the actual production situation. The rationality and feasibility of this method are verified by predicting the motion precision and reliability of the gear transmission system.

In the future researches, we will further research the error synthesis mechanism of meta-action chain and the assembly precision prediction method of chain based on the research of meta-action unit. The prediction model of assembly error will be improved in follow-up researches.

Acknowledgments This work was supported in part by the National Natural Science Foundation of China under Grants 51835001 and 51705048, in part by the National Major.

Authors' contributions X.Y. conceived of the presented idea. X.Y. developed the theory and performed the computations. Z.W. and Z.M. verified the analytical methods. Y.R. and G.Z. supervised the findings of this work. All authors discussed the results and contributed to the final manuscript.

Funding This research received no external funding

Data availability All data generated or analyzed during this study are included in this article.

Compliance with ethical standards

Conflicts of interest The authors declare no conflict of interest.

References

1. Xiong Z, Wang H, Cao T, Yuan X, Yao C, Zhang Z, Zhou M, Ma G (2015) Error analysis on assembly and alignment of laser optical unit. Adv Mech Eng 7:168781401559574
2. Ni J, Tang W, Xing Y (2018) Assembly process optimization for reducing the dimensional error of antenna assembly with abundant rivets. J Intell Manuf 29:245–258
3. Li X, Yan K, Lv Y, Yan B, Dong L, Hong J (2019) Study on the influence of machine tool spindle radial error motion resulted from bearing outer ring tilting assembly. Proc Inst Mech Eng Part C J Mech Eng Sci 233:3246–3258
4. Zhong X, Liu H, Mao X, Li B, He S (2019) Influence and error transfer in assembly process of geometric errors of a translational axis on volumetric error in machine tools. Measurement 140:450–461
5. Shi X, Tian X, Wang G, Zhang M, Zhao D (2018) A simplified model for assembly precision information of complex products based on tolerance semantic relations. Sustainability 10(12):4482
6. Easum J, Nagar J, Werner P, Werner D (2018) Efficient multiobjective antenna optimization with tolerance analysis through the use of surrogate models. IEEE Trans Antennas Propag 66:6706–6715
7. He C, Zhang S, Qiu L, Liu X, Wang Z (2019) Assembly tolerance design based on skin model shapes considering processing feature degradation. Appl Sci 9:3216
8. Whitney D, Gilbert O, Jastrzebski M (1994) Representation of geometric variations using matrix transforms for statistical tolerance analysis in assemblies. Proc IEEE Int Conf Rob Autom 6:191–210
9. Zhou S, Liu Z, Tan J (2011) Assembly sequence deviation transfer model and quality evaluation method based on dimension variation. Chin J Mech Eng 47:1–8
10. Zhang T, Zhang Z, Jin X, Ye X, Zhang Z (2016) An innovative method of modeling plane geometric form errors for precision assembly. Proc Inst Mech Eng Part B J Eng Manuf 230:1087–1096
11. Zhang Z, Zhang Z, Jin X, Zhang Q (2018) A novel modelling method of geometric errors for precision assembly. Int J Adv Manuf Technol 94:1139–1160
12. Mao J, Chen D, Zhang L (2016) Mechanical assembly quality prediction method based on state space model. Int J Adv Manuf Technol 86:107–116
13. Wang X, Liu M, Ge M (2016) Optimization method of assembly quality control valve for complex mechanical products based on hybrid particle swarm optimization. J Mech Eng 52:130–138
14. Du Q, Zhai X, Wen Q (2018) Study of the ultimate error of the axis tolerance feature and its pose decoupling based on an area coordinate system. Appl Sci 8:435
15. Zhao Q, Guo J, Hong J (2018) Assembly precision prediction for planar closed-loop mechanism in view of joint clearance and redundant constraint. J Mech Sci Technol 32:3395–3405
16. Hu J, Zhang Y, Ge M, Liu M, Liu C, Wang X (2016) Optimal control method on assembly precision for a remanufactured car engine based on state space model. Assem Autom 36:460–472

17. Saravanan A, Jerald J (2019) Ontological model-based optimal determination of geometric tolerances in an assembly using the hybridised neural network and Genetic algorithm. J Eng Des 30: 180–198
18. Sun W, Mu X, Sun Q, Sun Z, Wang X (2018) Analysis and optimization of assembly precision-cost model based on 3D tolerance expression. Assem Autom 38:497–510
19. Ran Y, Zhang G, Zhang L (2016) Quality characteristic association analysis of computer numerical control machine tool based on meta-action assembly unit. Adv Mech Eng 8:2071832022
20. Li Y, Zhang G, Wang Y, Zhang X, Ran Y (2019) Research on reliability allocation technology for NC machine tool meta-action. Qual Reliab Eng Int 35:2016–2044
21. Yu H, Zhang G, Ran Y, Li M, Jiang D, Chen Y (2019) A Reliability allocation method for mechanical product based on meta-action. IEEE Trans Reliab 69:373–381
22. Fan J, Wang P, Zhang H, Ma N, Yin J (2019) Research on tolerance modeling method and 3D tolerance analysis technology based on STD. IOP Conf Ser Mater Sci Eng 493:12050
23. Sergent A, Bui M, Favreliere H, Duret D, Samper S, Villeneuve F (2011) Identification of machining defects by Small Displacement Torsor and form parameterization method. Proceedings of IDMME 22:1–6
24. Wang X, Liu M, Ge M, Ling L, Liu C (2015) Research on assembly quality adaptive control system for complex mechanical products assembly process under uncertainty. Comput Ind 74:43–57
25. Che H, Zeng S, Guo J (2019) Reliability assessment of man-machine systems subject to mutually dependent machine degradation and human errors. Reliab Eng Syst Saf 190:106504
26. Desrochers A, Riviere A (1997) A matrix approach to the representation of tolerance zones and clearances. Int J Adv Manuf Technol 13(9):630–636
27. Chen H, Jin S, Li Z, Lai X (2015) A modified method of the unified Jacobian-Torsor model for tolerance analysis and allocation. Int J Precis Eng Manuf 16(8):1789–1800
28. Chen H, Jin S, Li Z, Lai X (2015) A solution of partial parallel connections for the unified Jacobian-Torsor model. Mech Mach Theory 91:39–49
29. Chen H, Tang G, Li Z, Jin S (2014) Three-dimensional tolerance analysis of engine based on Jacobian-Torsor statistical model. Harbin Gongcheng Daxue Xuebao 35(11):1397–1402
30. Wu D, Coatanea E, Wang GG (2019) Employing knowledge on causal relationship to assist multidisciplinary design optimization. J Mech Des Trans ASME 141(4)
31. Jin S, Hua C, Li Z, Lai X (2015) A small displacement torsor model for 3D tolerance analysis of conical structures. J Mech Eng Sci 229(14):2514–2523
32. Rao S, Bhatti P (2001) Probabilistic approach to manipulator kinematics and dynamics. Reliab Eng Syst Saf 72:47–58